

## Ordered Phases of Diblock Copolymers in Selective Solvent

Gregory M. Grason

Department of Physics and Astronomy, University of Pennsylvania, Philadelphia, PA 19104-6396, USA  
Dated: October 30, 2019

We propose a mean-field model to explore the equilibrium coupling between micelle aggregation and lattice choice in neutral copolymer and selective solvent mixtures. We find both thermotropic and lyotropic transitions from face-centered cubic to body-centered cubic ordered phases of spherical micelles. This transition is controlled entirely by the increasing length scale of intermicelle repulsions, suggesting that lattice entropy does not play a large role in lattice choice in this system. These results shed new light on the relationship between micelle structure (‘crew cut’ or ‘hairy’) and long-range order in micelle solutions.

Well known for their ability to self-assemble into a seemingly endless array of nanoscale structures [1], neutral diblock copolymer and solvent mixtures have recently received significant attention as a test bed for phenomena of a more classical nature: the crystallization of spherical particles [2, 3, 4, 5, 6, 7, 8]. In selective solvent copolymer chains aggregate into spherical micelles, protecting the insoluble polymer blocks. At high concentrations the swollen coronal brushes of neighboring micelles come into contact. To minimize the repulsive effect of this contact, the micelles adopt lattice configurations: generically, so-called ‘crew cut’ micelles with short coronal brushes favor the fcc structure, while so-called ‘hairy’ micelles with larger coronae favor the bcc lattice arrangement [2, 3, 5]. In a series of systematic studies, Lodge and coworkers identified fcc-bcc transitions with increasing temperature,  $T$  [4, 7], and polymer concentration, [5, 6]. Monte Carlo simulations of solutions of star polymers with effective repulsions [9] held at fixed number density,  $n$ , and aggregation number,  $p$ , predict that a low fcc-bcc transition occurs with decreasing  $p$  [10], in qualitative agreement with experiments in micelle solutions [7, 8]. However, in copolymer solutions  $p$  and  $n$  are determined thermodynamically, and the relationship between this work and equilibrium observations is so far unclear.

In this Letter we employ a mean-field model to probe the relationship between the thermodynamics of micelle aggregation and lattice choice in copolymer solutions at fixed temperature and concentration. This approach combines treatments of good and bad solvent polymer brushes with an effective theory for the free-energy cost from interactions and entropy of confining micelles within a lattice. Our study addresses the following two questions, simultaneously: how do changes in micelle structure drive the fcc-bcc transition, and how does that structure respond to lattice confinement? While the ‘crew cut’ vs. ‘hairy’ micelle distinction roughly describes ordered phase behavior, we find that the relative sizes of corona and core do not wholly determine lattice choice. Both thermotropic and lyotropic fcc-bcc transitions are controlled by an increase in density on the scale of the intermicelle potential,  $(2R_0)$ , the micelle size.

When the reduced density,  $\eta = n(2R_0)^3$ , rises above a critical value, micelle interactions favor the bcc structure over fcc. Whereas the thermodynamics of hard sphere systems is determined only by lattice entropy [11], in this system lattice choice is driven by micelle interactions.

We consider a solution of diblock copolymer chains composed of  $N_A$  insoluble A segments and  $N_B$  soluble B segments. Each chain segment has length,  $a$ , and volume,  $a^3$ , equal to the volume of a solvent (S) molecule. The specific A-B, A-S and B-S repulsions are characterized by the respective Flory parameters,  $A_{AB}$ ,  $A_{AS}$  and  $A_{BS}$  [12]. In the absence of any intermicelle effects, we consider three contributions to the cost of creating a micelle:  $F_A$  the core free energy,  $F_B$  the corona free energy and  $F_{int}$  the free energy of the core/corona interface. Assuming a small, uniform fraction of solvent,  $\chi_A$ , in the core we have the mean-field free energy of the inner domain,

$$F_A = \frac{3^2 p}{80} \frac{R_A^2}{N_A a^2} + p N_A \frac{A}{(1 - \chi_A)} \ln \chi_A + A_{AS} \chi_A ; \quad (1)$$

where  $R_A$  is the radius of the micelle core (see Fig 1 inset) and all energies are measured in units of  $k_B T$ . The first term is the free energy of a strongly-stretched swollen

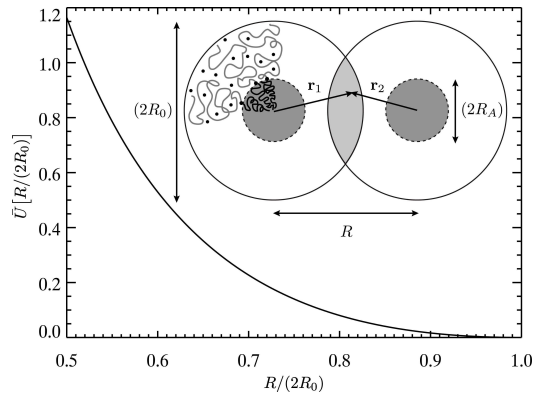


FIG. 1: The computed interaction between two copolymer micelles of diameter  $(2R_0)$ . The strength of the repulsion scales as  $p^{3/2} (k_B T)$ . The volume of increased osmotic pressure due to the coronal overlap is shown as light gray. Both potential and force go to zero as  $R \rightarrow (2R_0)$ .

polymer brush [13], and the second is simply the mixing free energy of the domain. From volume considerations we have,  $(4 = 3)R_A^3 = pN_A = (1 - \alpha_A)$ . To model the B polymer brush, we use the Daudin and Cotton scaling model for star polymers [14]. Here, the corona is a semi-dilute solution where the polymer "blob" size is a function of radial distance,  $r = \sqrt[3]{4/p}$ . From good-solvent scaling we have radial the dependence of polymer density in the corona,  $\rho_B(r) = \frac{1}{r^3} p^{2/3} = r^{4/3}$  [15], where  $\alpha = 1 - 2\alpha_B$  is the dimensionless excluded volume parameter for the B segments [12]. In this domain, the free energy scales as the number of blobs, and it is straightforward to compute [15, 16] that  $F_B = (p^{3/2} - \frac{1}{4}) \ln R_0/R_A$  where  $\alpha$  is some unknown number of order unity. The microcell size is set by the relation  $R_0^{5/3} = R^{5/3} + R_A^{5/3}$  where  $R$  is the size of a star polymer brush in the limit of a vanishing core [15] for which it can be shown,  $R = N_B^{3/2} p$ .

At the interface these two domains come into contact, and across the interface the densities of each component will adjust to reach the limiting values on either side. For example, from inside to outside the solvent fraction rises from  $\alpha_A$  to  $\alpha_B = 1 - \alpha_B(R_A)$ . Qualitatively, we expect that the free energy cost of creating such an interface is dominated by the increased exposure of A monomer to solvent. Here, we propose a simplified approach to estimating the surface tension. Assuming the polymer density is sufficiently high to justify a mean-field treatment [12], we estimate the effect of the interface by allowing for a region of finite width,  $w$ , where the A, B and solvent densities take on their average intermediate values. Relative to an infinitely sharp interface ( $w = 0$ ) the mixing free-energy cost of such an interfacial region can be written roughly as  $\sigma_A w (1 - \alpha_{eff})$ , where  $\alpha_{eff}$  is the area of the interface,  $\alpha_{eff} = (A_B - A_A)/2$  is the average solvent fraction and

$$\alpha_{eff} = \frac{A_B (1 - \alpha_A) (1 - \alpha_B)}{2 A_S (1 + \alpha_A) + B_S (1 - \alpha_B) - 2^2 \frac{(1 - \alpha_A)(1 - \alpha_B)}{w}}; \quad (2)$$

where  $2 = (B_A - A_B) = (1 - \alpha_A)$ . We estimate the chain entropy using the following argument. At the interface the polymer chains loop back and forth in the presence of the composition gradients, but on scales smaller than the interface width the chain correlations should be unaffected by composition. We then imagine dividing the interface into Gaussian blobs of size,  $w$ , each representing a  $k_B T$  of free energy. To compute the free-energy cost, we count the total number of blobs. There are roughly  $\sigma_A w (1 - \alpha_{eff})$  total segments at the interface and each blob contains  $(w/a)$  segments. Thus, the presence of interface costs roughly  $\sigma_A w (1 - \alpha_{eff}) (a^2/w)$  in free energy, due to chain correlations. Combining the two effects and minimizing over interface width we find an estimate for the interfacial tension,  $\sigma = \sigma_A w (1 - \alpha_{eff})^{1/2}$ . The total free energy due to the interface in the microcell is sim-

ply,  $F_{int} = 4 R_A^2 \sigma$ . The virtue of this result is that in the zero solvent limit the expression for  $\sigma$  reduces to the well-known surface tension between two molten polymer domains [17]. Although the molten polymer scaling may not be strictly applicable for these solvent conditions, we expect that this mean-field approach captures the qualitative dependence of the surface tension on the polymer solubility and solvent content.

We consider the cost of bringing two microcells to a separation,  $R < (2R_0)$ , with their coronae in contact (see Fig. 1). We model the two-body interaction,  $U(R)$ , by computing the increase in osmotic pressure introduced by brush overlap. Using the  $\frac{9}{4}$  scaling of osmotic pressure [12] and the density profile of star polymers we have,

$$U(R) = \left( (\alpha_0)^2 \right)^{1/3} \frac{dV}{\text{over}} \left( \rho_B(r_1) + \rho_B(r_2) \right)^{9/4} \frac{p^{3/2} h}{4} \frac{R}{(2R_0)}^i; \quad (3)$$

where the integral is carried out over the overlap volume of the coronae. We factor out the  $p$ -dependent strength of the interaction and the scaled interaction,  $U(R) = (2R_0)$  is shown in Fig. 1. While overlapped conformation should relax to lower interpenetration [16], we expect this calculation to provide a realistic account of free energy of interaction. Since the  $p^{3/2}$  scaling of the potential and concave shape ( $d^2U/dR^2 > 0$ ) are preserved by this approach, our results would be qualitatively similar if we adopted the modified logarithmic potential [9, 15]. Computing the average interaction energy of competing lattice arrangements proceeds straightforwardly for this nited-range potential. Using the fact that a fraction of the solution,  $\alpha$ , is polymer and assuming that each microcell has aggregation number,  $p$ , we find,

$$n = \frac{0}{p(N_A + N_B)} : \quad (4)$$

Since separations between lattice sites grow as  $n^{1/3}$ , the average interaction energy depends only on  $p$  and the reduced density,  $\rho = n/(2R_0)^3$ .

Before treating the lattice fluctuations we make a few comments about the "potential" energy of various cubic structures. In addition to the fcc and bcc structures, we compute the free energy of simple cubic, diamond and A15 structures. Microcell interactions only contribute when the size ( $2R_0$ ) has reached the nearest-neighbor separation,  $R_{nn}$ . Because fcc has the highest close-packing density,  $\frac{f_{\text{cc}}}{c_p} = 1/4$ , the potential energy prefers this structure for low reduced density (at fixed  $p$ ). However, above a critical density of  $\rho = 2/14$ , the potential energy of the bcc lattice drops below that of the fcc. While the location of the fcc-bcc crossover is sensitive to the details of the interaction, the high-density preference of the bcc structure is generic. Indeed, this crossover occurs for a

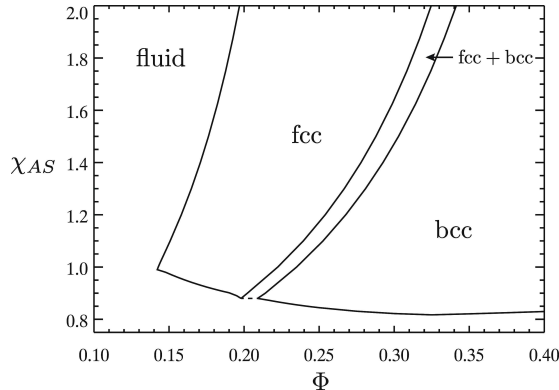


FIG. 2: The mean-field phase diagram for a solution of  $N_A = N_B = 50$  copolymer chains. A coexistence region is shown between the fcc and bcc phases. The region where the fluctuations are greater than 10% of the nearest-neighbor distance is labeled as the uid m iocelle phase.

broad range of concave potentials, such as Yukawa interactions [19, 23]. In the relevant density range, 1  $\leq \Phi \leq 5$ , the potential energy (and ultimately the total free energy) of the other structures is greater than fcc or bcc, and only the A15 lattice, with its open structure [18], comes within even 5% of the best structure.

To model the free-energy contributions from positional fluctuations of the m iocelle we adopt the Einstein description and compute the cost of displacing the m iocelles from equilibrium in the presence of the potential produced by lattice neighbors fixed at their equilibrium positions:

$U = (1/2) \sum_i \sum_i (r_i)^2$  [20]. The harmonic restoring coefficients,  $\epsilon_i$ , depend on the lattice and derivatives of the potential. The equilibrium free-energy contribution per m iocelle is given by,

$$F_{\text{fluct}} = \frac{1}{2} \sum_i \epsilon_i = \frac{1}{2} \sum_i \epsilon_i \ln \epsilon_i = \frac{1}{2} \sum_i \epsilon_i \ln h(r_i)^2 \epsilon_i ; \quad (5)$$

where equipartition gives  $h(r_i)^2 \epsilon_i = \epsilon_i^{-1}$ . While the approach is approximate [22], it allows us to apply directly Lindemann's criterion to assess crystal melting [21]. Moreover, this model predicts that fcc-bcc differences in lattice entropy, which depend only on  $\epsilon$ , are not larger than  $0.5k_B$  per m iocelle, in reasonable agreement with predictions for other soft systems [20, 23]. In comparison, the potential energy difference between fcc and bcc at typical parameter ranges reaches well above  $10 \text{ (} k_B T \text{)}$  per m iocelle. Lattice entropy differences are small on this scale and ultimately do not play a significant role in the fcc-bcc transition for this system. The translational degrees of freedom are simply too few in comparison to the many chain degrees of freedom in the coronalbrushes [18].

Combining the energetics of the m iocelle structure with the cost of constraining the m iocelles in a lattice, we minimize the intensive free energy over m iocelle degrees of free-

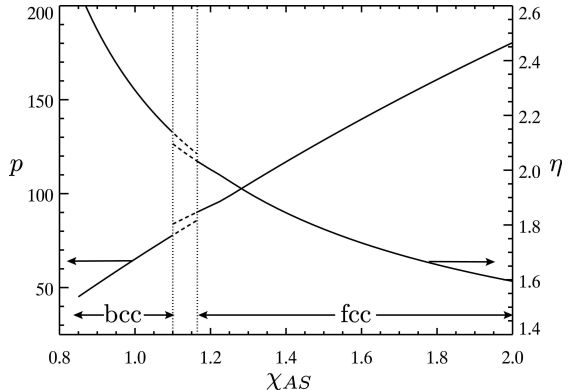


FIG. 3: The average aggregation number and reduced density of the  $N_A = N_B = 50$  copolymers at  $\epsilon = 0.25$ . The fcc+bcc coexistence region is delimited by vertical dotted lines.

dom,  $p$  and  $\eta$ , to obtain the mean-field behavior. We set the value of  $\epsilon$  by forcing the crystal to melt below  $p = 40$ , to match the observations of ref. [7]. We expect the thermodynamics to depend most strongly on the solvent selectivity,  $\chi_{AS}$  (which decreases with  $T$ ); thus, we set  $\chi_{AB} = 0.1$  and  $\chi_{BS} = 0.3$ . Fig. 2 shows the  $\chi_{AS}$  phase diagram for a solution of  $N_A = N_B = 50$  copolymers. The model predicts a low concentration fcc phase and high concentration bcc phase separated by a narrow coexistence region. We note that the positive curvature of the fcc-bcc phase boundary in  $\chi_{AS}$  plane reflects the shape of the boundary observed in controlled  $T$  and experiments [5, 6].

In Fig. 3 we plot mean values  $p$  and  $\eta$  through the thermotropic (decreasing  $\chi_{AB}$ ) transition, for a  $\epsilon = 0.25$  solution. Scaling arguments at low concentration predict that aggregation grows with surface tension  $\sigma = \epsilon^{1/2} N_A^{1/3}$  [16], and although growth is modified by interactions, we find the same qualitative behavior at higher concentration. As  $\chi_{AS}$  (and  $\epsilon$ ) decrease, we see that  $p$  also decreases, leading to an increased density,  $\eta$ , from eq. (4). And while decreased  $p$  reduces m iocelle size, increased solvent content in the core tends to keep the m iocelle size fairly constant. When  $\chi_{AS}$  is decreased from 2 to 1 (assuming a segment size of  $a = 5 \text{ \AA}$ )  $R_0$  only decreases from  $13.4 \text{ nm}$  to  $10.8 \text{ nm}$ , a change of 20%, while over the same range  $p$  falls by 64%. This increases the reduced density,  $\eta$ , from 1.59 to 2.29, passing through the fcc-bcc potential energy crossover density. We note the model predicts a fcc-bcc transition at  $p = 80$  and  $\chi_{AB} = 0.26$ , agreeing very closely with structural observations from Lodge et al. of a 25% neutral copolymer solution [7].

The appearance of a high- $T$  bcc m iocelle lattice has been attributed to the Alexander-Mc唐ue argument for crystals near melting [24]. However, this mean-field model gives rather unambiguous evidence that the bcc m iocelle lattice is stable at high temperature due to the long range of m iocelle repulsions for large  $\chi_{AS}$ . While the fcc-

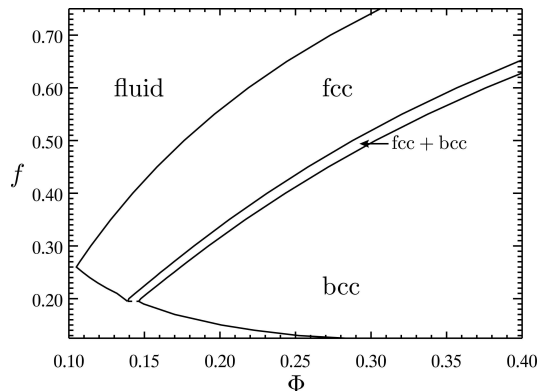


FIG. 4: The mean-field phase diagram for solutions of  $N_A + N_B = 100$  copolymers at  $\alpha_S = 1.5$  as function of  $\Phi$  and polymer architecture,  $f = N_A/(N_A + N_B)$ .

bcc crossover for systems with concave, repulsive interactions is quite generic [19, 23], it is not clear how this fact relates to the geometric features of the reciprocal lattice stabilizing bcc near melting. These results also demonstrate that while micelle interactions may become short-ranged, the micelles do not behave as hard spheres, and as such we cannot attribute fcc stability to entropy of the micelle center-of-mass [11]. The fcc micelle lattice is stable precisely where the potential energy of fcc and bcc lattice diagram is.

The lyotropic transition proceeds similarly. Doubling from 0.2 to 0.4 at  $\alpha_S = 1.5$ , only weakly increases  $p$  and  $R_0$ , 15% and 5%, respectively. Consequently,  $p$  increases almost two-fold from 1.45 to 2.80, again driving the fcc-bcc transition. The slight increase in  $p$  over this range is driven both by interactions and lattice entropy. Both micelle repulsions and the potential restraining micelle fluctuations decrease as  $f$  is reduced, lowering the free energy. Since  $d = dp = p$ , the strength of both effects is dependent, leading to feedback between increased and increased  $p$ .

Finally, we investigate the influence of copolymer architecture on lattice structure. In Fig. 4 we plot the fixed temperature ( $\alpha_S = 1.5$ ) mean-field phase diagram for block copolymer solutions as a function of  $f$  and A-polymer fraction,  $f$ . Generally, the low  $f$  (long B block) chains prefer the bcc structure, since the large coronas are large and the interactions are longer range. Likewise, micelles with larger cores for high  $f$ , prefer the fcc structure. However, micelle structure does not uniquely determine lattice structure. Rather "hairy" micelles of  $f = 0.25$  chains with a corona height to core size ratio of  $H_B = R_A \approx 1.86$  assume the fcc structure below  $\Phi \approx 0.17$ , while "crew cut" micelles of  $f = 0.6$  chains with  $H_B = R_A \approx 0.63$  assume the bcc arrangement above  $\Phi \approx 0.38$ . Clearly, the micelles interaction cannot "know" about the core size, since interactions take place

at the brush tips where physics is governed by the local blob size,  $r = p$ . In principle, all fcc-bcc transitions should occur at some critical  $\Phi$ , independent of temperature, chain architecture and concentration. However, it may not be possible to determine the size,  $(2R_0)$ , of highly overlapping micelles with sufficient precision to resolve this critical reduced density experimentally.

We have described a simple, mean-field model which unifies the description of the thermotropic and lyotropic fcc-bcc transition in copolymer and selective solvent mixtures. Indeed, the accuracy of these predictions can be traced to the generic, geometric principle driving the fcc-bcc crossover for particles with concave repulsions.

It is a pleasure to thank J. Bang, R. Kamien, P. Zherl and C. Santangelo for helpful discussions. This work was supported by NSF Grant DMR-01-02459, the Donors of the Petroleum Research Fund, Administered by the American Chemical Society and a gift from L.J. Bernstein.

---

- [1] D. E. Discher and A. Eisenberg, *Science* 297, 967 (2002). S. Jain and F. S. Bates, *Science* 300, 460 (2003).
- [2] G. A. M. Connell, et al., *Phys. Rev. Lett.* 71, 2102 (1993).
- [3] G. A. M. Connell and A. P. Gast, *Phys. Rev. E* 54, 5447 (1996).
- [4] J. Bang, et al., *Phys. Rev. Lett.* 89, 215505 (2002).
- [5] T. P. Lodge, et al., *Macromolecules* 35, 4707 (2002).
- [6] J. Bang, et al., *J. Chem. Phys.* 121, 11489 (2004).
- [7] T. P. Lodge, et al., *Phys. Rev. Lett.* 92, 145501 (2004).
- [8] M. Laurati, et al., *Phys. Rev. Lett.* 94, 195504 (2005).
- [9] C. N. Likos, et al., *Phys. Rev. Lett.* 80, 4450 (1998).
- [10] M. Watzlawek, et al., *Phys. Rev. Lett.* 80, 4450 (1999).
- [11] B. J. Alder, et al., *J. Chem. Phys.* 49, 3688 (1968).
- [12] P.-G. de Gennes, *Scaling Concepts in Polymer Physics*, Cornell University Press: Ithaca, 1979.
- [13] A. N. Semenov, *Sov. Phys.-JETP* 61, 733 (1985).
- [14] M. Daoud and J. P. Cotton, *J. Phys. (Paris)* 43, 531 (1982).
- [15] T. A. Witten and P. A. Pincus, *Macromolecules* 19, 2509 (1986).
- [16] T. M. Birshtein and E. B. Zhulina, *Polymer* 30, 170 (1989).
- [17] E. Helfand and A. M. Sapozhnikov, *J. Chem. Phys.* 62, 1327 (1975).
- [18] P. Zherl and R. D. Kamien, *Phys. Rev. Lett.* 85, 3528 (2000).
- [19] J. K. Klemmer, et al., *Phys. Rev. Lett.* 57, 2694 (1986).
- [20] M. O. Robbins, et al., *J. Chem. Phys.* 88, 3286 (1988).
- [21] F. A. Lindemann, *Z. Phys.* 11, 609 (1910).
- [22] When  $R_{nn} > (2R_0)$ , we estimate  $h(r_i)^2 \propto r_i^{-2}$  as the sum of fluctuation magnitude for  $R_{nn} = (2R_0)$  and the displacement needed to make nearest-neighbor contact.
- [23] D. Hone, et al., *J. Chem. Phys.* 79, 1474 (1983).
- [24] S. Alexander and J. M. Cates, *Phys. Rev. Lett.* 41, 702 (1978).